NATIONAL ADVISORY COMMITTEE FOR AERONAUTICS

TECHNICAL NOTE

No. 1309

CORRELATION OF TWO EXPERIMENTAL METHODS OF DETERMINING THE ROLLING CHARACTERISTICS OF UNSWEPT WINGS

By Robert MacLachlan and William Letko

Langley Memorial Aeronautical Laboratory
Langley Field, Va.

Washington
May 1947

NATIONAL ADVISORY COMMITTEE FOR AERONAUTICS

TECHNICAL NOTE NO. 1309

CORRELATION OF TWO EXPERIMENTAL METHODS OF DETERMINING THE ROLLING CHARACTERISTICS OF UNSWEPT WINGS

By Robert MacLachlan and William Letko

SUMMARY

The rolling moments of one tapered wing and two geometrically similar rectangular wings were measured both in rolling flow with the wing stationary and in straight flow with forced rotation of the wing to obtain a correlation between the two methods of testing and to determine the rolling characteristics of the wings.

The results showed that for unswept wings the rolling characteristics (the rate of change of rolling-moment coefficient and the rate of change of aileron hinge-moment coefficient with rolling velocity) obtained by rotation of the air agreed with those obtained by forced rotation of the wing. Calculated values of the rolling characteristics of the three wings checked closely the experimental values. The calculations showed that, for the wings tested, the variation of damping in roll with angle of attack depends primarily on the variation in the slope of the lift curve with angle of attack. The results also showed that, when the wing was yawed, the values of the damping in roll and of the variation of aileron hinge moment with roll were approximately proportional to the square of the cosine of the angle of yaw.

INTRODUCTION

In order to predict either the dynamic stability of an airplane or the airplane motions resulting from movement of the lateral controls, accurate values of the dynamic lateral-stability derivatives of the airplane must be known. Included in the present investigation are two methods by which the derivatives resulting from roll may be measured. The first of these methods, which has in the past been used by the National Advisory Committee for Aeronautics, provides for forced rotation of the model in a straight air stream. The second method provides, instead, for rotation of the air stream (rolling flow) with the model fixed. In order to obtain a correlation between the results obtained by these two methods, a tapered wing and

two geometrically similar rectangular wings of different span were tested both in rolling flow with the wing stationary and in straight flow with forced rotation of the wing. The rolling-flow method does not exactly simulate the conditions of an airplane in steady roll or the conditions of the model in forced rotation. With rolling flow there is a variation of static pressure with distance from the center of rotation to balance the centrifugal force caused by the air rotation. Such a condition does not exist for the case of an airplane in steady roll or for model rotation. If the body to be tested is symmetrical, any forces resulting from the pressure gradient should cancel. The pressure gradient, however, tends to cause an inward flow in the boundary layer of the wing, which might be expected to alter the characteristics of the various sections along the span of the wing. The investigation was therefore made to determine whether this effect would cause any appreciable change in the damping in roll of unswept wings. The two rectangular wings of different span were tested so that an indication of the uniformity of rolling flow across the tunnel could be obtained.

SYMBOLS

α angle of attack, degrees

ψ angle of yaw, degrees

C_h aileron hinge-moment coefficient $\left(\frac{\text{Hinge moment}}{qc_a^2b_a}\right)$

ΔC_h increment of aileron hinge-moment coefficient

C_l rolling-moment coefficient $\left(\frac{\text{Rolling moment}}{qSb}\right)$

ΔC_l increment of rolling-moment coefficient

C_{l_p} damping coefficient; that is, rate of change of rolling-moment coefficient with wing-tip helix angle in radians $\left(\frac{\partial C_l}{\partial\left(\frac{pb}{2V}\right)}\right)$

$\frac{pb}{2V}$ wing-tip helix angle, radians

$\Delta\frac{pb}{2V}$ increment of wing-tip helix angle, radians

C_{h_p} rate of change of hinge moment with wing-tip helix angle $\left(\frac{\partial C_h}{\partial (pb/2V)}\right)$

C_{h_α} rate of change of aileron hinge moment with angle of attack, per degree $\left(\frac{\partial C_h}{\partial \alpha}\right)$

c_{l_α} section lift-curve slope, per degree

$(\alpha_p)_{C_h}$ absolute value of the ratio $\left|\frac{C_{h_p}}{C_{h_\alpha}}\right|$

δ_a aileron deflection (positive downward), degrees

b wing span, feet

b_a aileron span, feet

c_a aileron chord, feet

S area of wing, square feet

p rolling velocity, radians per second

V airspeed, feet per second

λ ratio of tip chord to root chord of wing

q free-stream dynamic pressure, pounds per square foot

R Reynolds number

APPARATUS AND TESTS

The tests were made in the 6-foot-diameter test section of the Langley stability tunnel which is illustrated in figure 1.

The model was mounted on a support which, when not locked, was free to rotate about the tunnel center line. For the forced rotation tests, the rate and direction of rotation of the model were regulated by changing the angle of attack of a small driving airfoil attached

to the support as shown in figure 2. For the rolling-flow tests the model was fixed and the air stream was rotated by means of the rotor shown in figure 3. This method has the advantage that all forces and moments can be measured with the model mounted on a conventional balance system.

Rolling moments were measured at various angles of attack and yaw for all the wings and, for the tapered wing, aileron hinge moments were also measured at zero aileron deflection. Rolling-moment readings were obtained from strain gages mounted on a beam which formed the junction between the model and the model support. The aileron hinge moments were also measured by strain gages.

The principal dimensions of the three wings tested are given in figure 4. Each of the models was made of laminated mahogany. The tapered wing was equipped with plain ailerons (fig. 4), to one of which was attached strain gages for hinge-moment measurement. The model configurations tested are given in table I.

The straight-flow tests with model fixed were made so that C_{h_α} could be obtained. All the tests were made at a dynamic pressure of 64.3 pounds per square foot which corresponds to test Reynolds numbers of about 1.02×10^6 for the 4-foot-span wings and 1.28×10^6 for the 5-foot-span wing.

RESULTS AND DISCUSSION

A preliminary investigation of the rotational distribution produced by the rolling-flow rotor indicated that the air-stream angle did not increase linearly with distance from the center of the tunnel. It was found, however, that, if the air-stream angles produced by positive and negative rotation were averaged, a nearly linear variation of air-stream angle with distance would be obtained. Because of warping of the rotor blades, however, the variation of air-stream angle at zero rotor speed was appreciable. In order to eliminate the effects of the variation of air-stream angle, the data obtained with air-stream rotation have been presented in the form of increments of C_l, C_h, and $pb/2V$. These increments were calculated by subtracting the values of C_l, C_h, and $pb/2V$ obtained with the smallest positive air-stream rotation from those obtained at the higher positive air-stream rotations and by averaging with these results the corresponding results produced by subtracting from the values obtained at the smallest negative air-stream rotation the values at higher negative air-stream rotations. These averaged increments are presented in figures 5 to 8 with additional points obtained

from model-rotation tests (both positive and negative model-rotation data have been plotted, by appropriate changes in sign, in the positive $\Delta pb/2V$ range). From these figures, values of C_{l_p} and C_{h_p} were measured for inclusion in figure 9 and table II, respectively. No wind-tunnel corrections were made to the data inasmuch as the lift coefficient was not measured; however, at a lift coefficient of 1.0, the angle-of-attack correction for the 5-foot-span wing was estimated to be about 1°.

Comparison of Forced-Rotation and Rolling-Flow Results

The C_{l_p} and C_{h_p} results obtained by the two experimental methods (figs. 5 to 8) showed consistent agreement, and indicated that, for unswept wings, the rolling-flow test procedure should be satisfactory.

A comparison of the results of the 4-foot- and 5-foot-span rectangular wings (fig. 9) showed very little difference in corresponding values of C_{l_p} and indicated that the uniformity of rolling flow across the tunnel was satisfactory for unswept wings of spans up to 5 feet.

Damping in Roll

The experimental values of C_{l_p} are plotted in figure 9 and are compared with values of C_{l_p} calculated from theoretical values of C_{l_p}/c_{l_α} given in figure 2 of reference 1 and from section lift data from the Langley two-dimensional low-turbulence tunnel. The section lift data for the two airfoil sections used are presented in figure 10 with additional curves showing the variation of section lift-curve slope c_{l_α} with angle of attack. In calculating the values of C_{l_p} the section lift-curve slope at each angle of attack was used. This method of calculation is approximate, particularly at the higher angles of attack, since, for a finite-span wing, the section lift-curve slope will not remain constant at all sections along the span of the wing. The agreement between the experimental and calculated curves (fig. 9) is generally considered fair and at small angles of attack is considered very good. For the wings tested, the variations in C_{l_p} with angle of attack are caused primarily by variations in the section lift-curve slope.

The damping in roll of the wings when yawed was found to be approximately proportional to $\cos^2\psi$ (fig. 11). This relation was expected,

since the velocity component normal to the leading edge varies as the cos ψ and, therefore, the dynamic-pressure component normal to the leading edge (to which the forces and moments are proportional) varies approximately as the $\cos^2\psi$.

Rate of Change of Aileron Hinge Moment with Rate of Roll

A calculated value of $(\alpha_p)_{C_h}$ for the aileron of the tapered wing was obtained by use of the information given in figures 3 and 4 of reference 1. The value obtained, 0.519, was then multiplied by values of C_{h_α} obtained from wind-tunnel tests of the tapered wing in straight flow (fig. 12) to give values for C_{h_p}. These values of C_{h_p}, together with the values obtained by the rolling-flow and forced-rotation tests, are presented in table II.

Because of the low magnitudes of C_{h_α} for this particular aileron-wing configuration, all the values of C_{h_p} were small. At an angle of 8° the values of C_{h_p} were generally higher than at zero angle of attack. This increase results from the increase in C_{h_α} as the angle of attack becomes higher. The value of C_{h_p} was found to be approximately proportional to $\cos^2\psi$ as was C_{l_p}.

CONCLUSIONS

The results of rolling-wing and rolling-flow tests on 4- and 5-foot-span rectangular wings and a 4-foot-span tapered wing in the Langley stability tunnel indicate the following general conclusions:

1. For unswept wings, the values of C_{l_p} and C_{h_p} (the rate of change of rolling-moment coefficient and the rate of change of aileron hinge-moment coefficient, respectively, with wing-tip helix angle) obtained by rotation of the air agreed with those obtained by forced rotation of the wing.

2. The values of C_{l_p} and C_{h_p} obtained checked closely with calculated values. The calculations showed that, for the wings tested, the variation of C_{l_p} with angle of attack depends primarily on the variation in the slope of the lift curve with angle of attack.

3. When the wing was yawed, the values of both C_{l_p} and C_{h_p} were approximately proportional to the square of the cosine of the angle of yaw.

Langley Memorial Aeronautical Laboratory
National Advisory Committee for Aeronautics
Langley Field, Va., April 4, 1947

REFERENCE

1. Swanson, Robert S., and Priddy, E. Laverne: Lifting-Surface-Theory Values of the Damping in Roll and of the Parameter Used in Estimating Aileron Stick Forces. NACA ARR No. L5F23, 1945.

TABLE I.- TEST PROGRAM

Tapered wing (δ_a = 0)	
α (deg)	ψ (deg)
Rolling flow	
a_0	0, 15, 30
2, 4, 6, a_8, 10, 12, 14, 16	0
Straight flow (model fixed)	
-2, 0, 2, 4, 6, 8, 10, 12	0, 15, 30

Rectangular wing	
α (deg)	ψ (deg)
Rolling flow; 4-ft span	
a_0	0, 15, 30
2, 4, 6	0
a_8	0, 15, 30
10, 12, 14, 16	0
Rolling flow; 5-ft span	
a_0, a_8	0

[a]Also tested with forced rotation of wing in straight flow

TABLE II.- AILERON HINGE-MOMENT VALUES FOR THE TAPERED WING

ψ (deg)	α (deg)	C_{h_α}	C_{h_p}	
			Theoretical	Experimental
0	0	-0.0021	-0.0011	-0.0012
0	8	-.0069	-.0036	-.0030
15	0	-.0020	-.0010	-.0011
30	0	-.0016	-.0008	-.0008

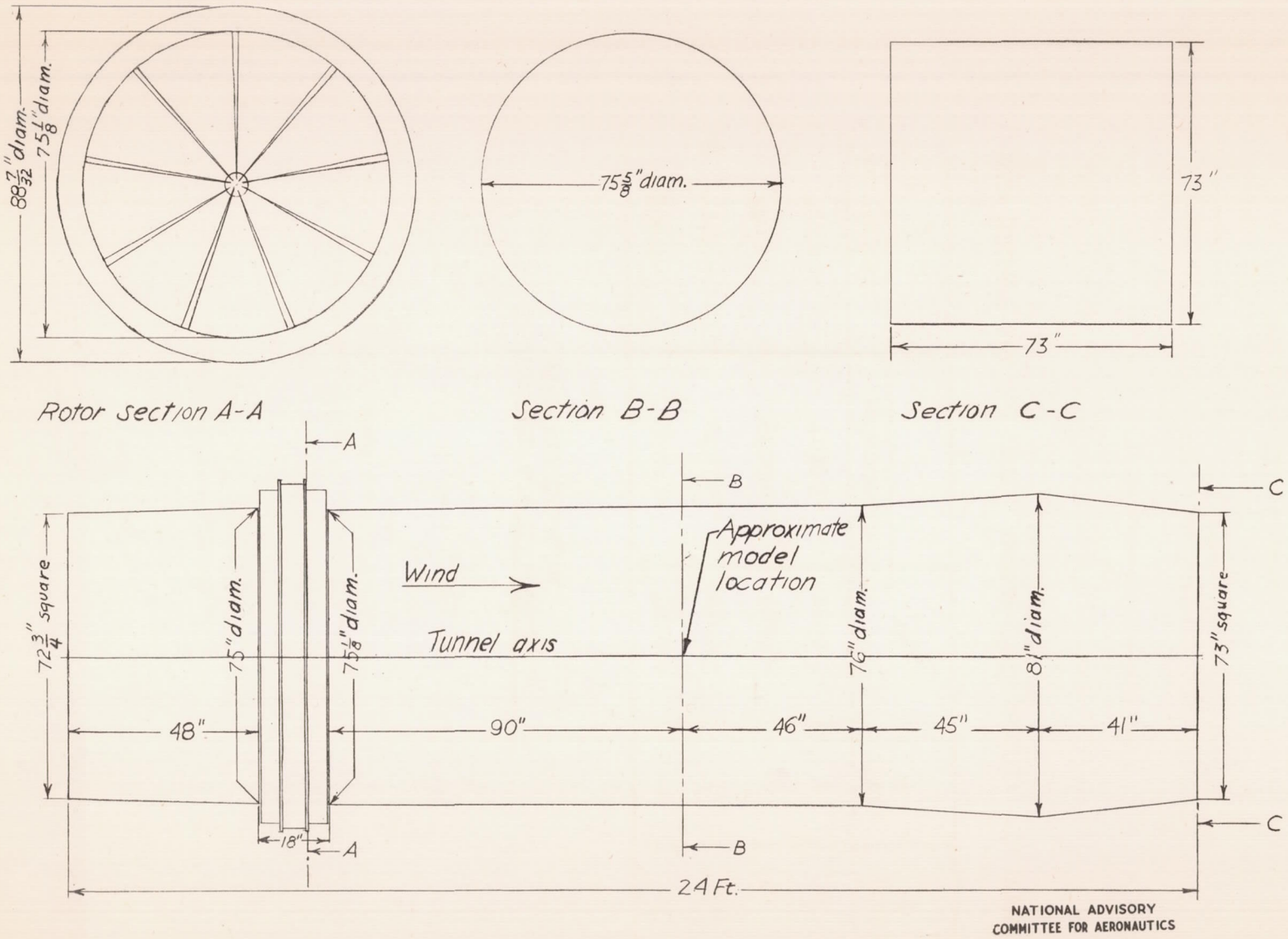

Figure 1.- Rolling-flow test section of the Langley stability tunnel.

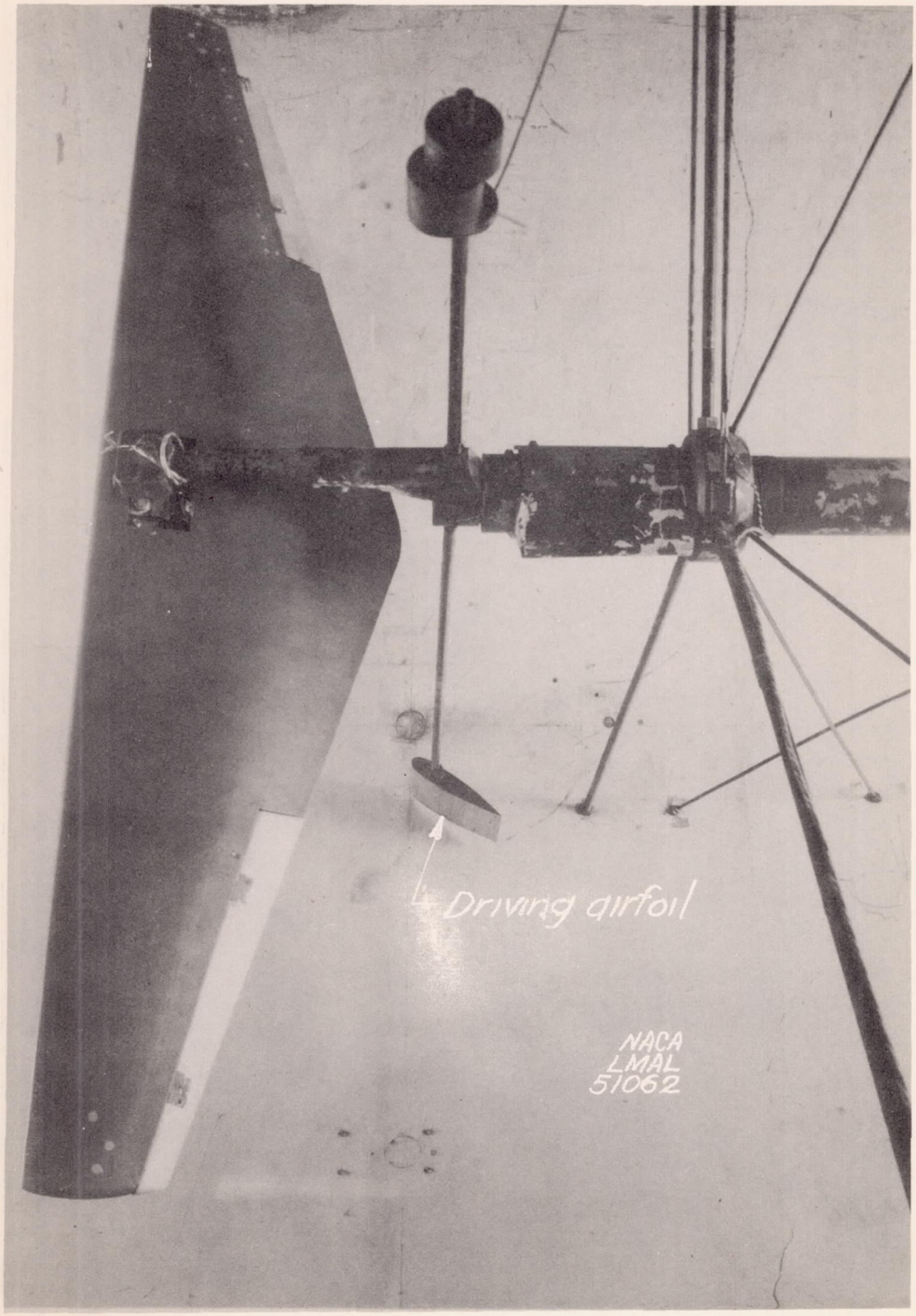

Figure 2.- View of 4-foot tapered model mounted in tunnel, showing small driving airfoil attached to model support.

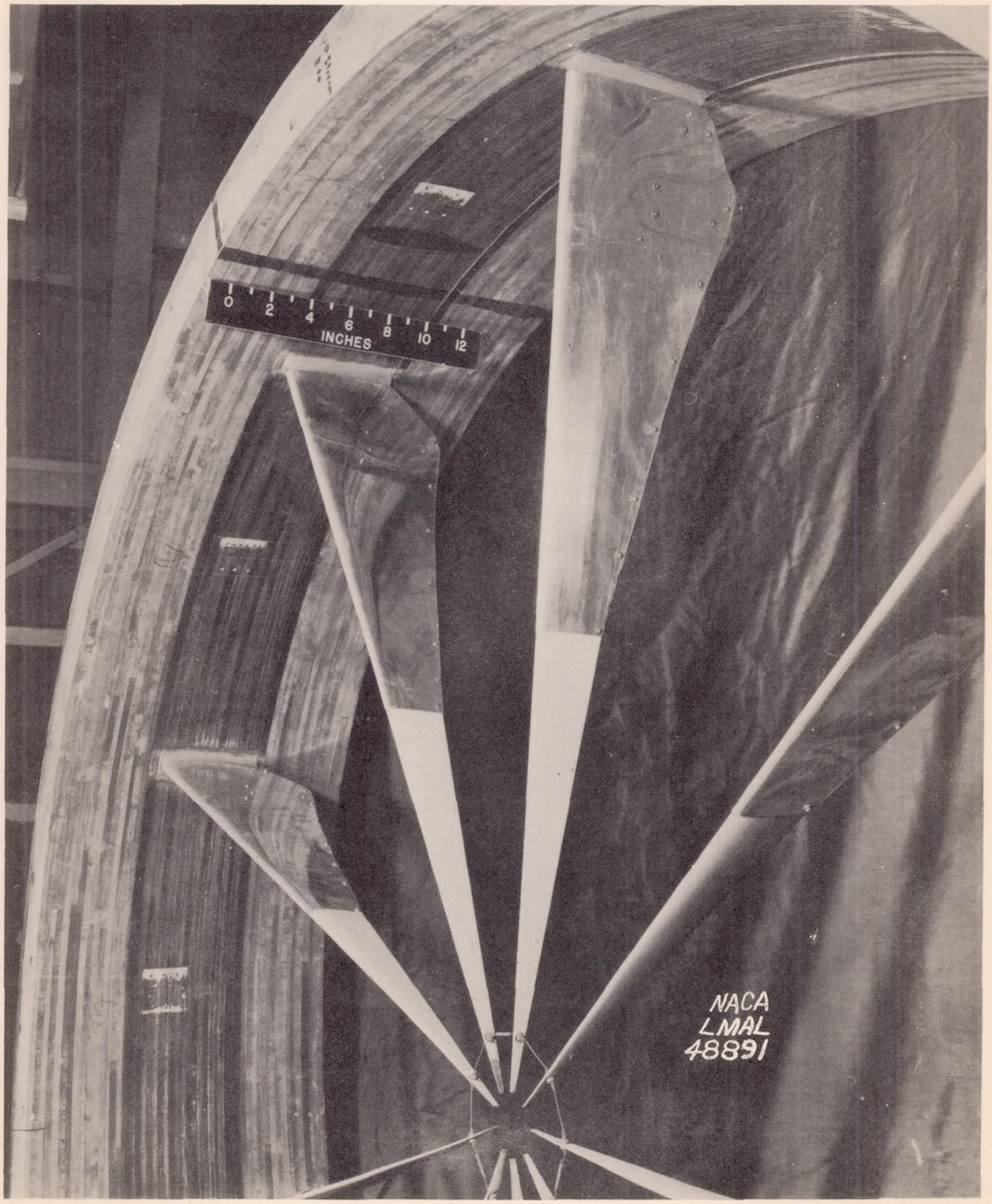

Figure 3.- Close-up view of rotor.

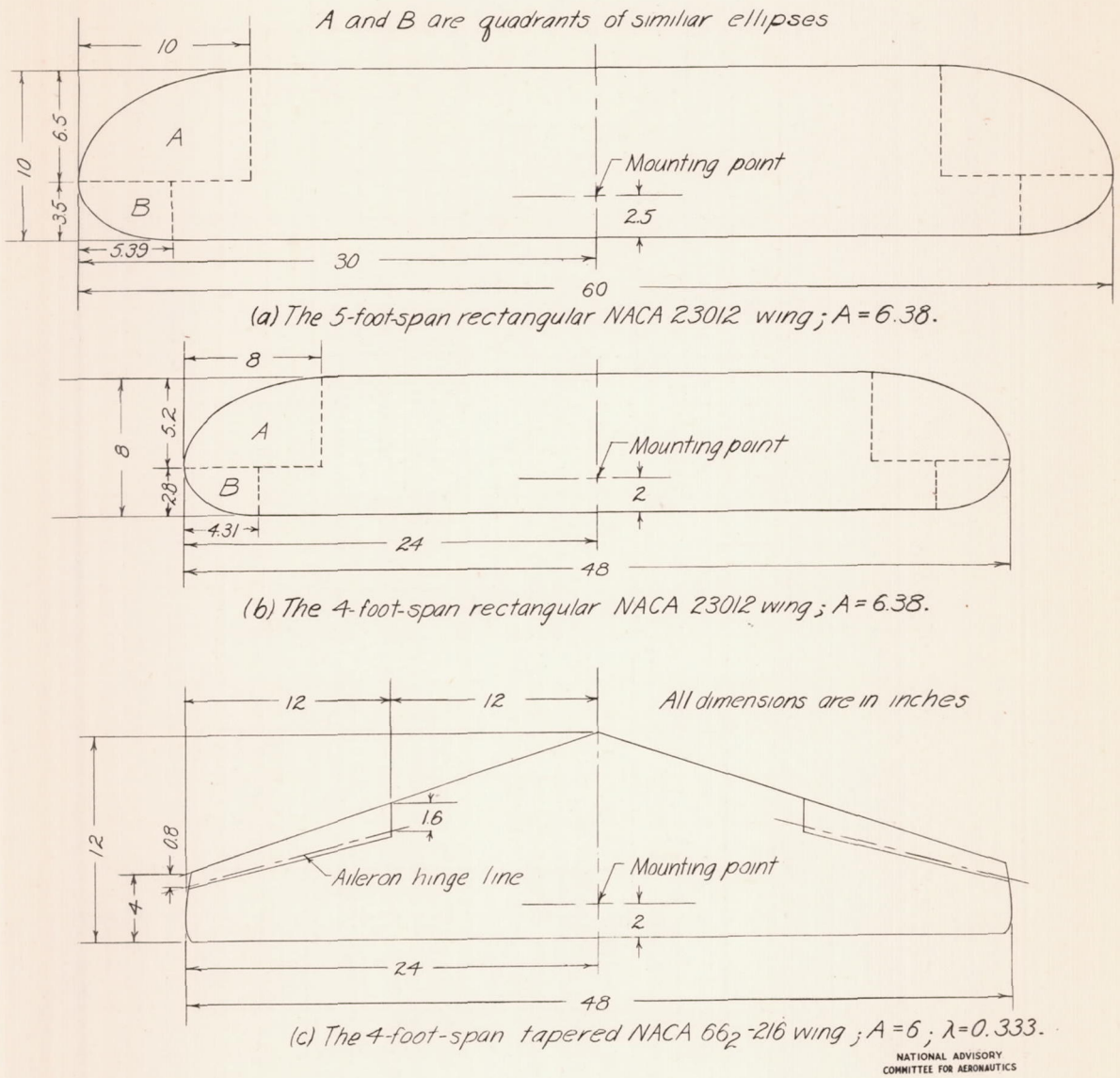

Figure 4.- Plan forms of wings tested.

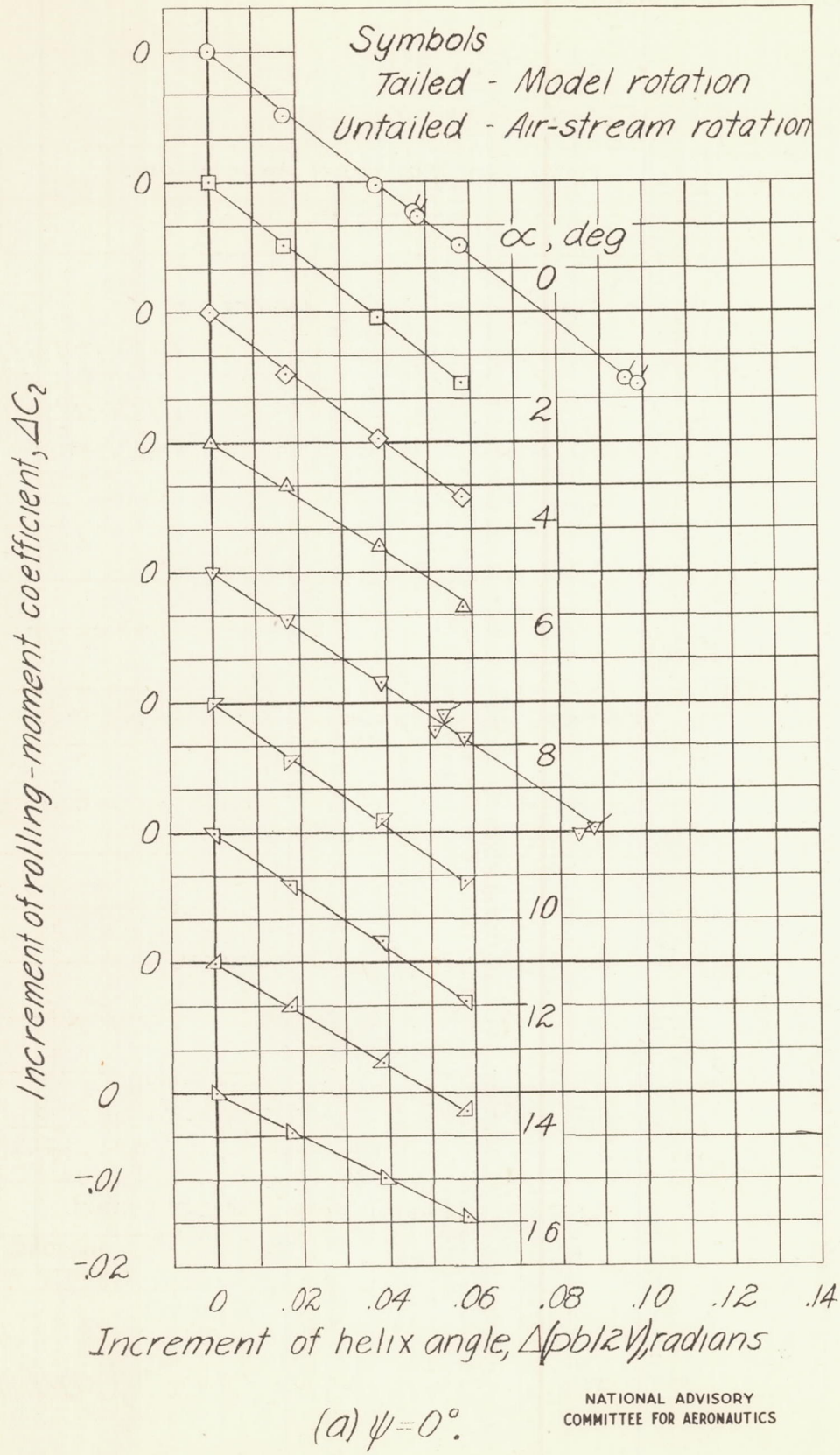

Figure 5.- Variation of rolling-moment coefficient with wing-tip helix angle. Tapered wing.

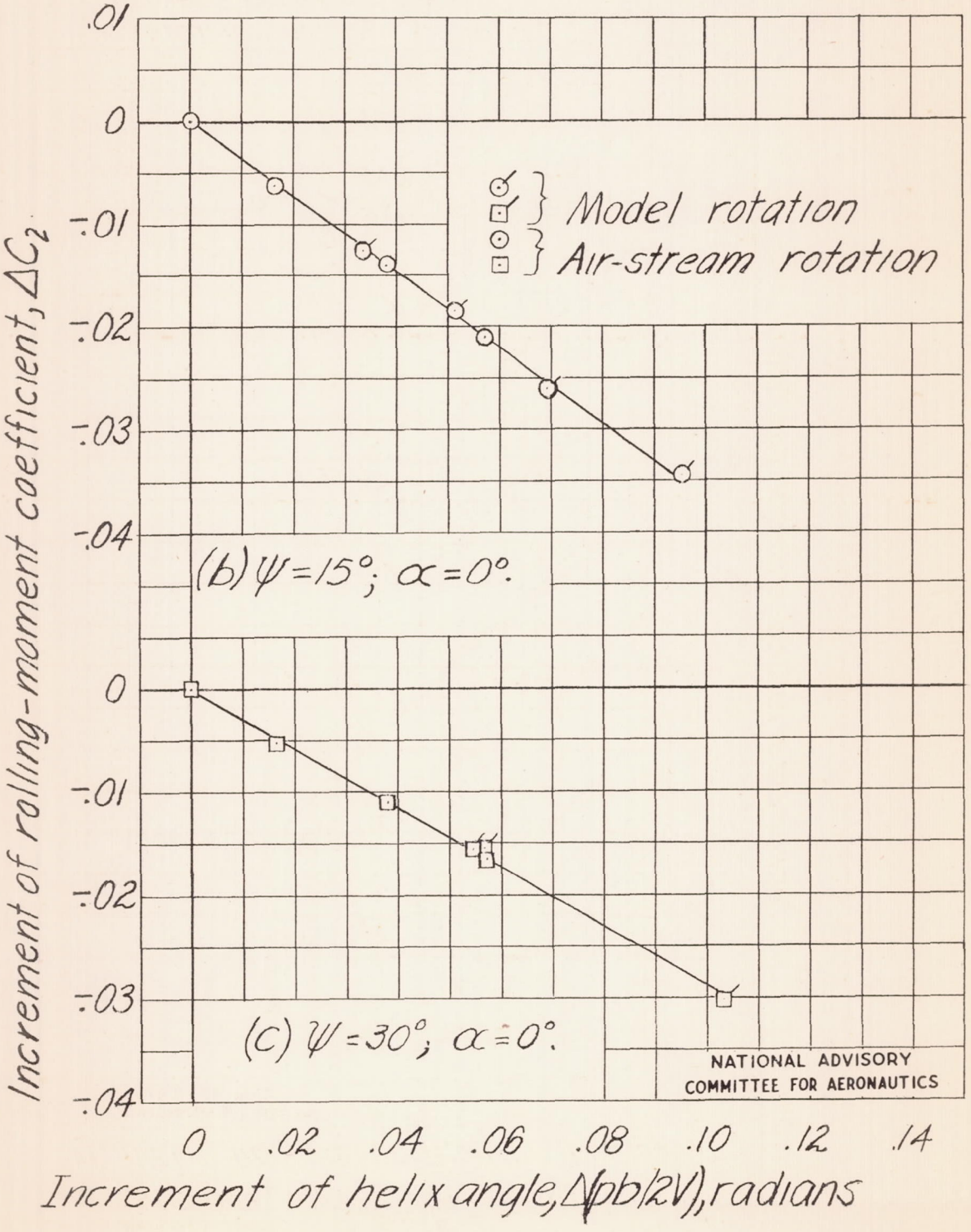

Figure 5.- Concluded.

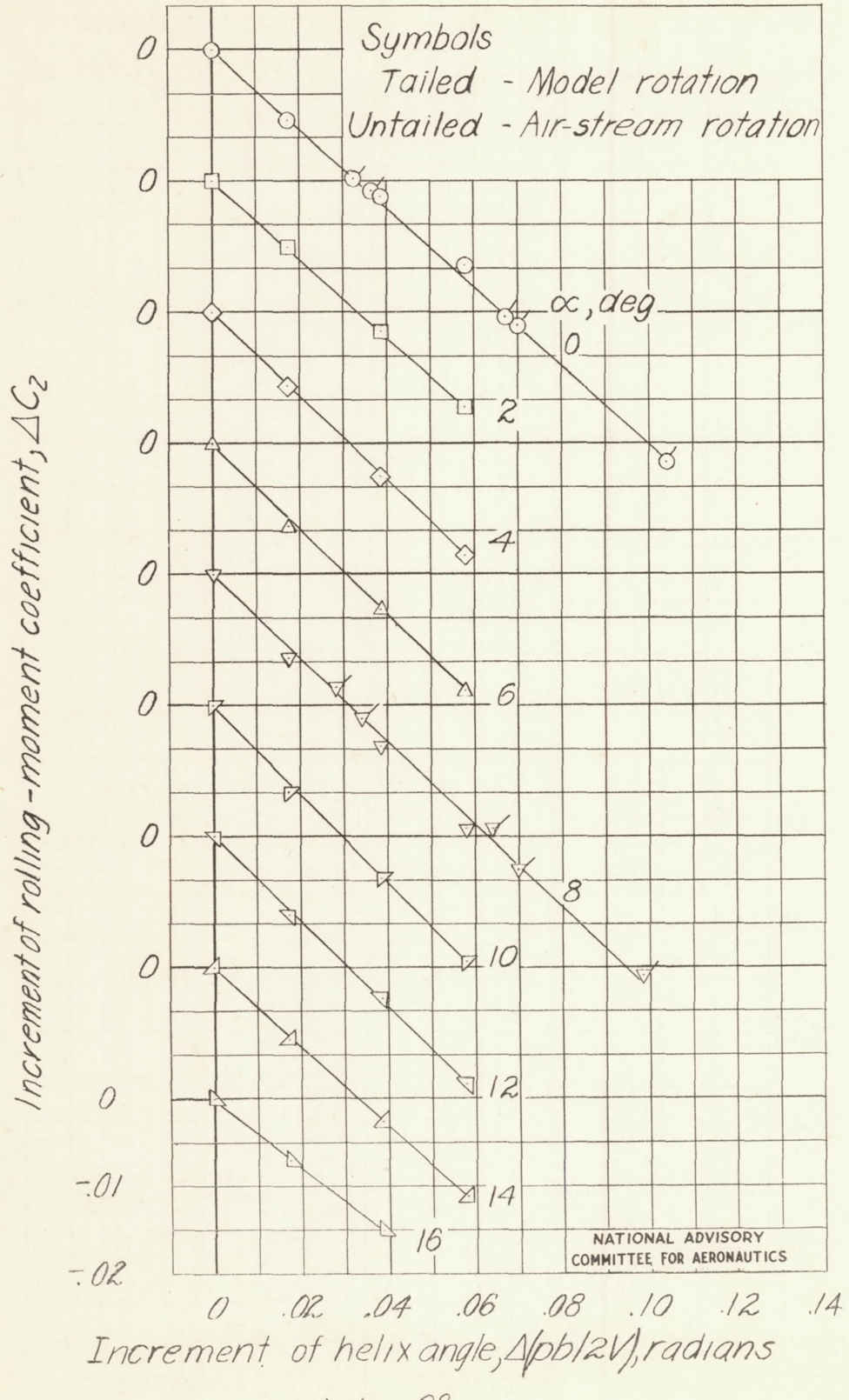

(a) $\psi = 0°$.

Figure 6.- Variation of rolling-moment coefficient with wing-tip helix angle. Four-foot-span rectangular wing.

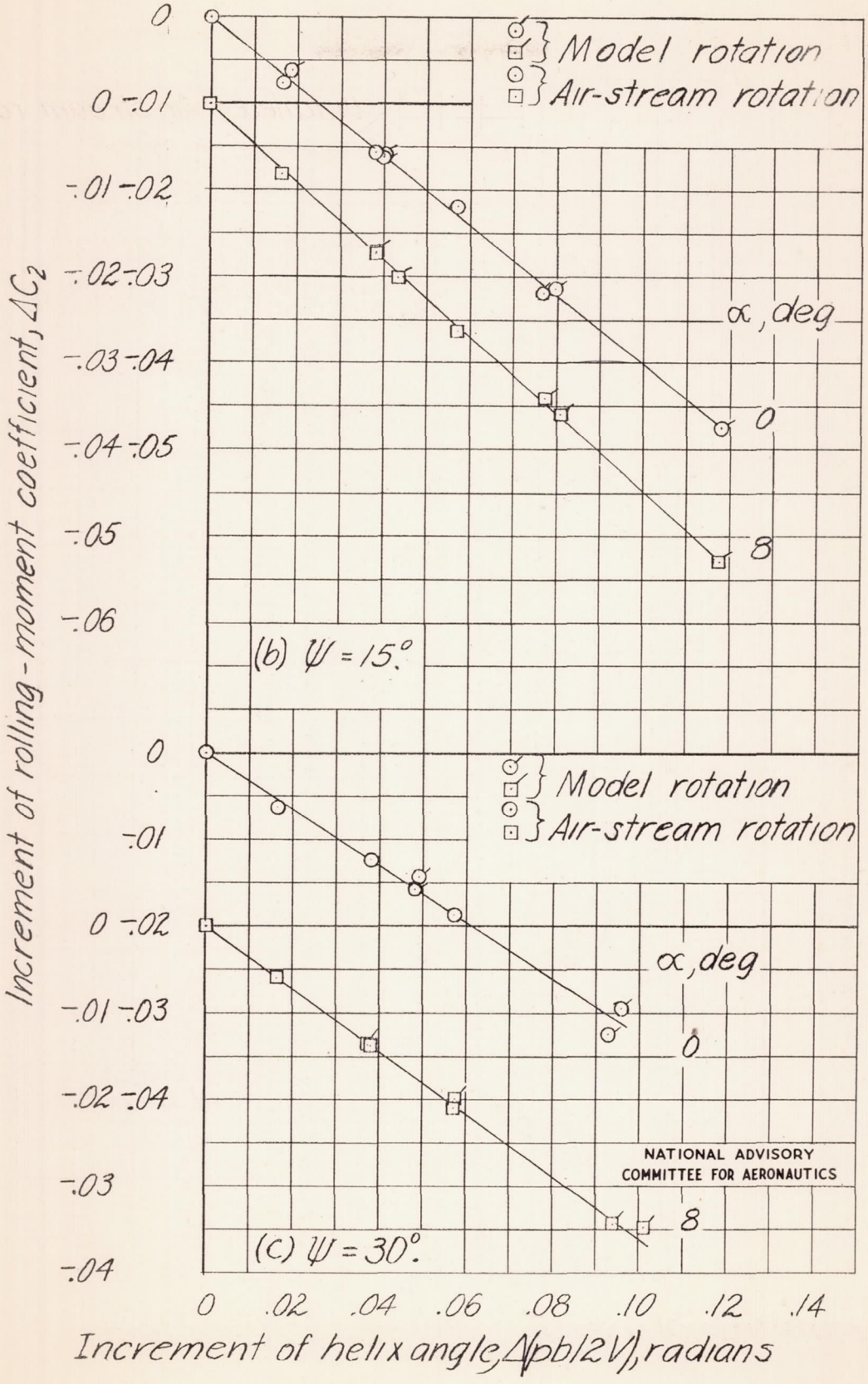

Figure 6.- Concluded.

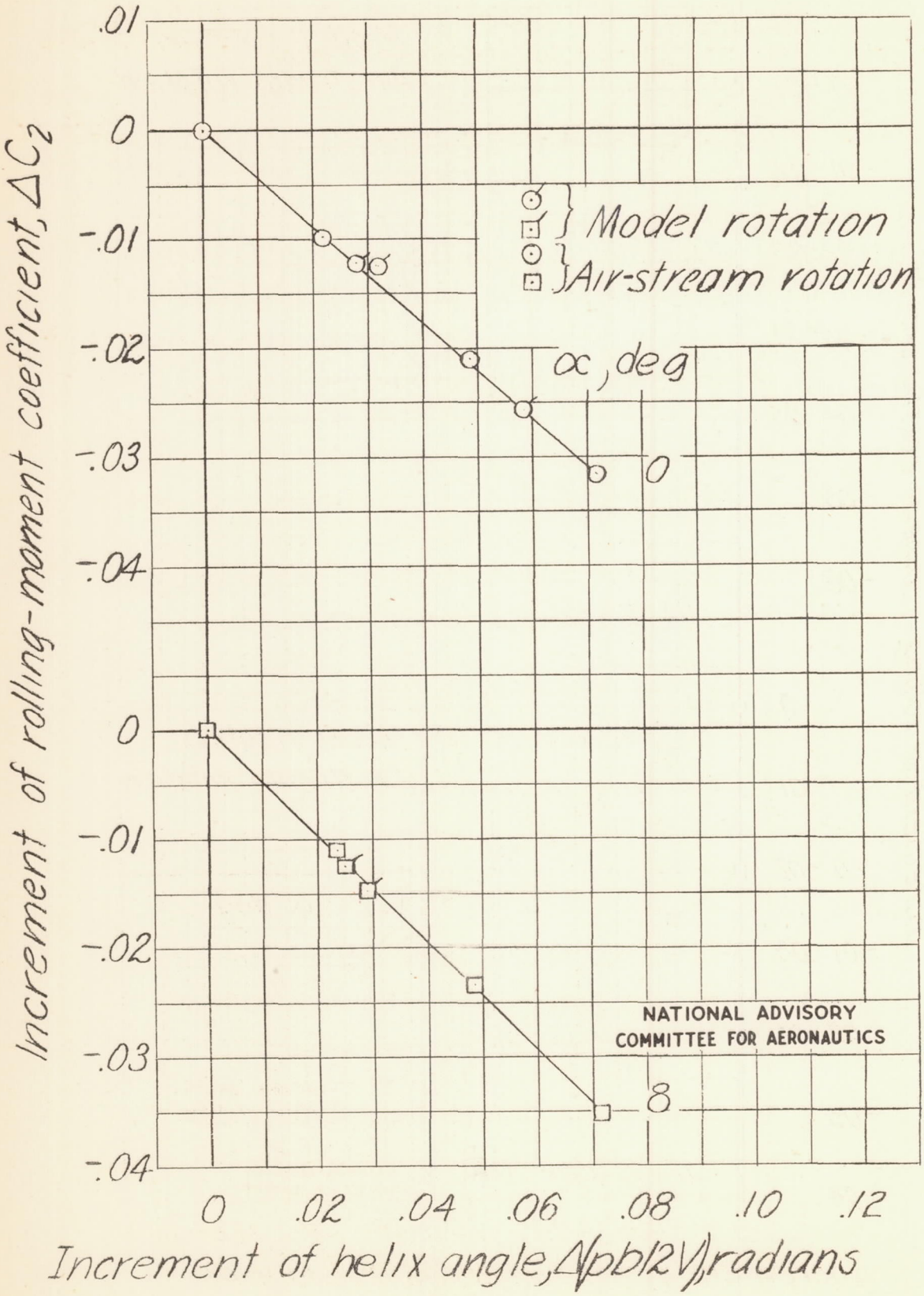

Figure 7.- Variation of rolling-moment coefficient with wing-tip helix angle. Five-foot-span rectangular wing; $\psi = 0^{\circ}$.

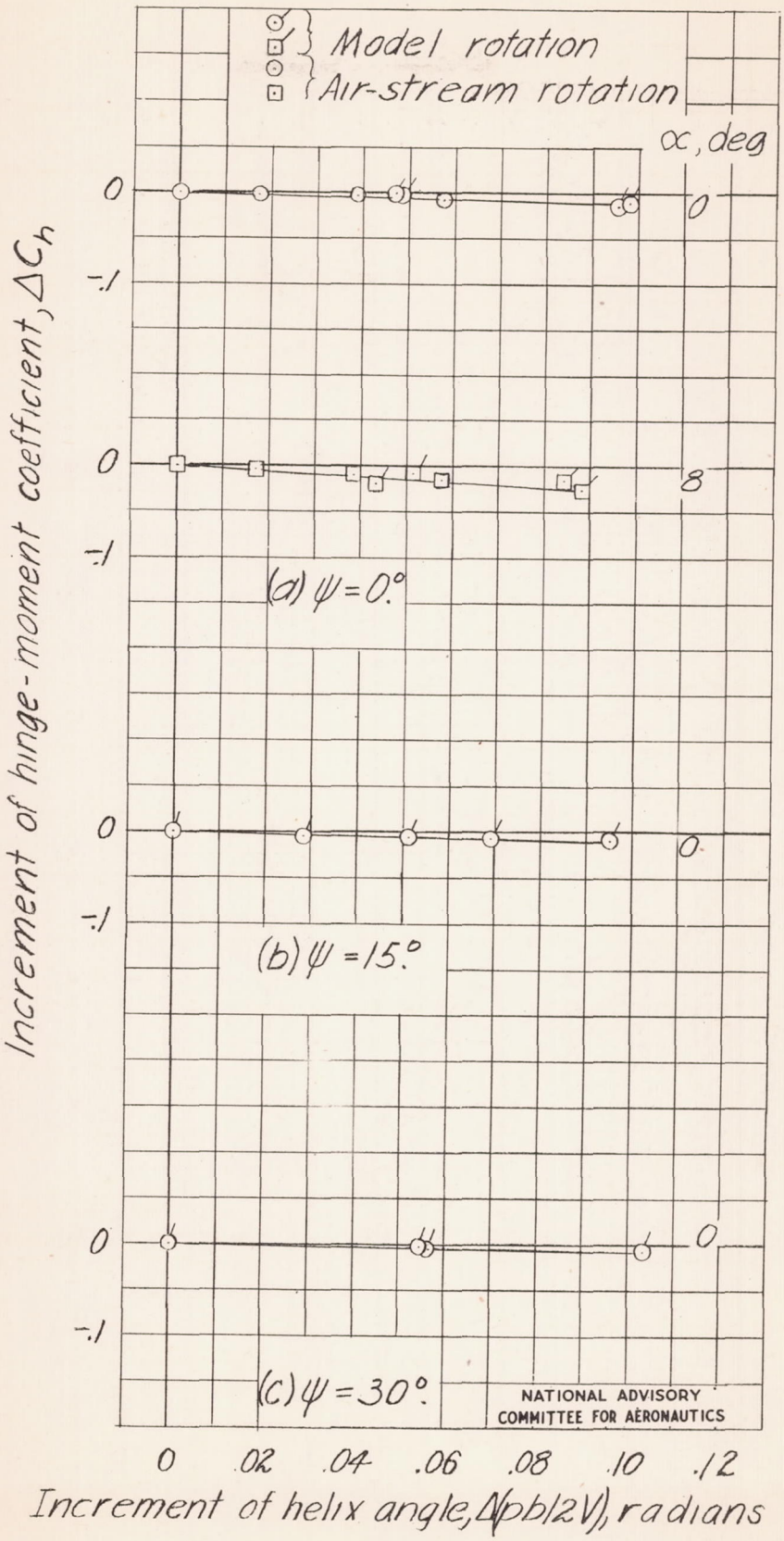

Figure 8.- Variation of aileron hinge-moment coefficient with wing-tip helix angle. Tapered wing; $\delta_a = 0^\circ$.

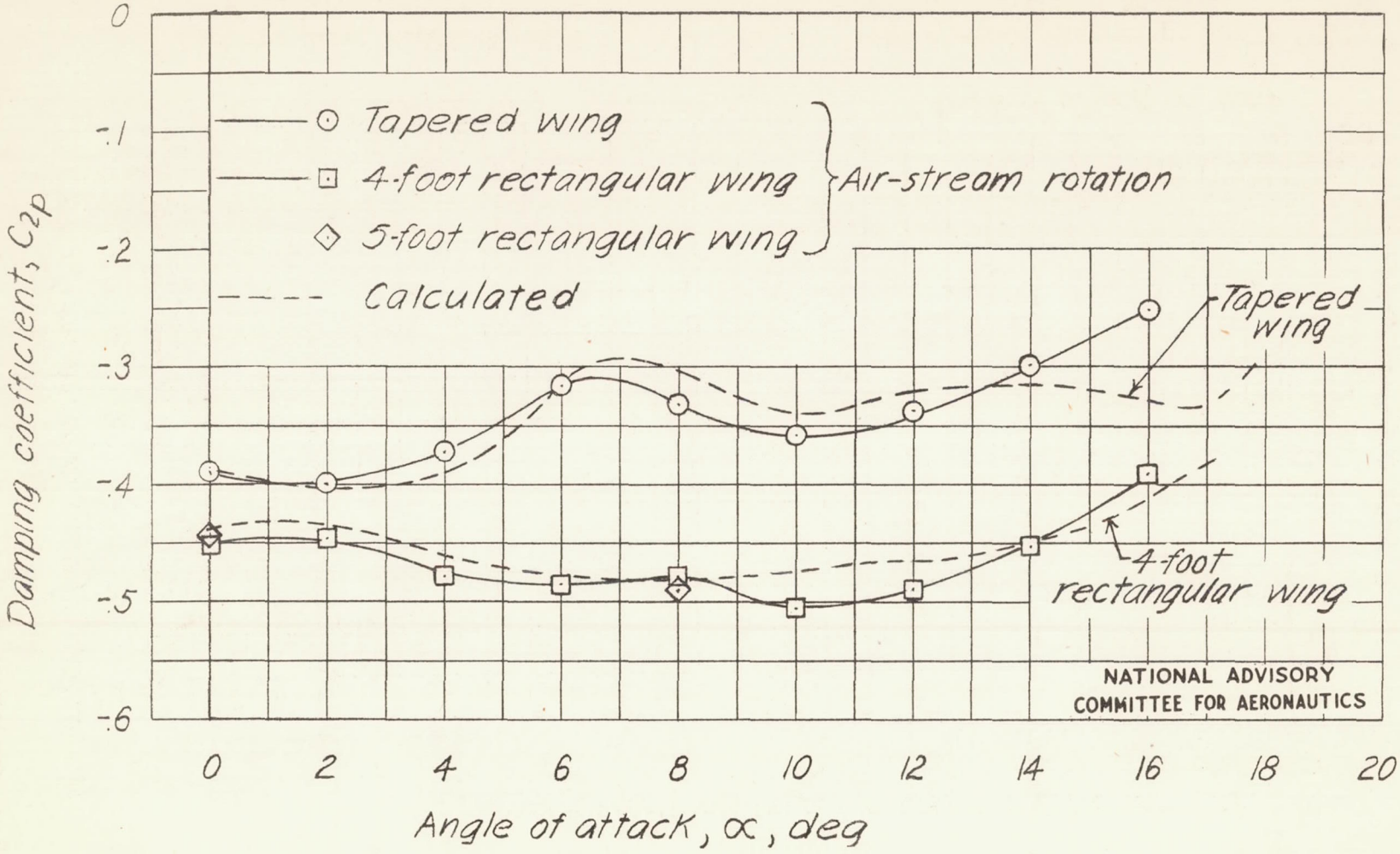

Figure 9.- Variation of damping in roll with angle of attack. $\psi = 0^{\circ}$.

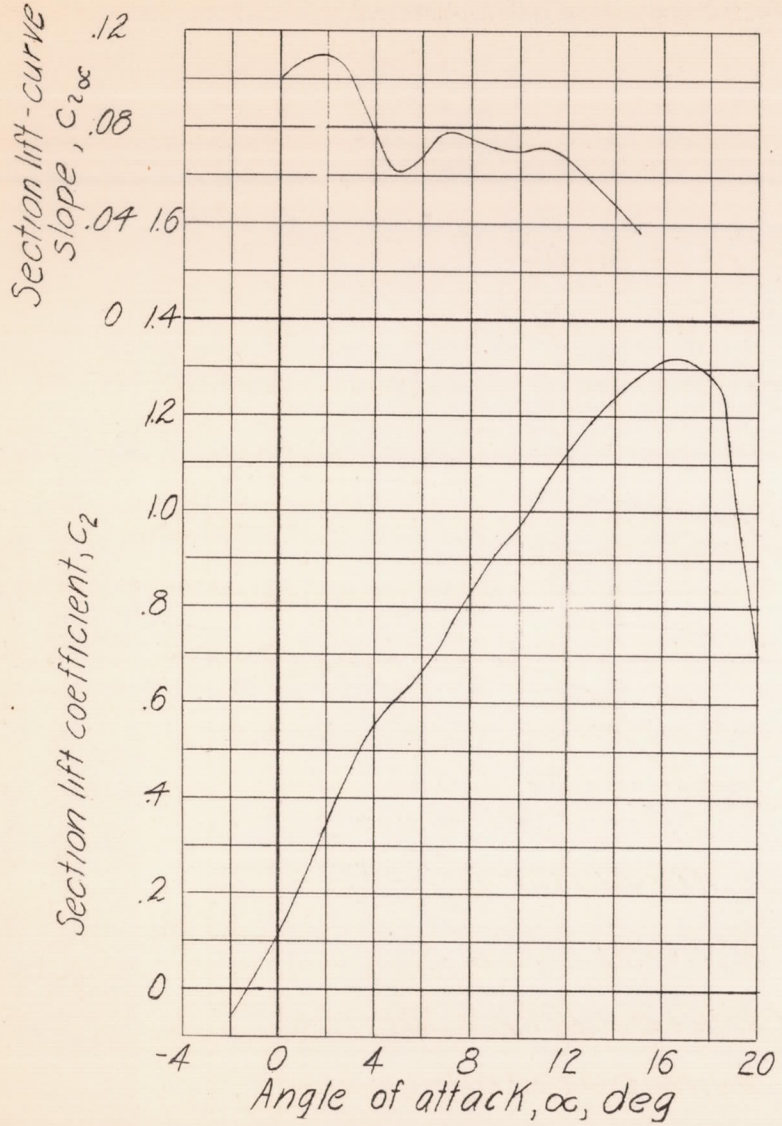

(a) Tapered wing; NACA 66_2-216 airfoil section.

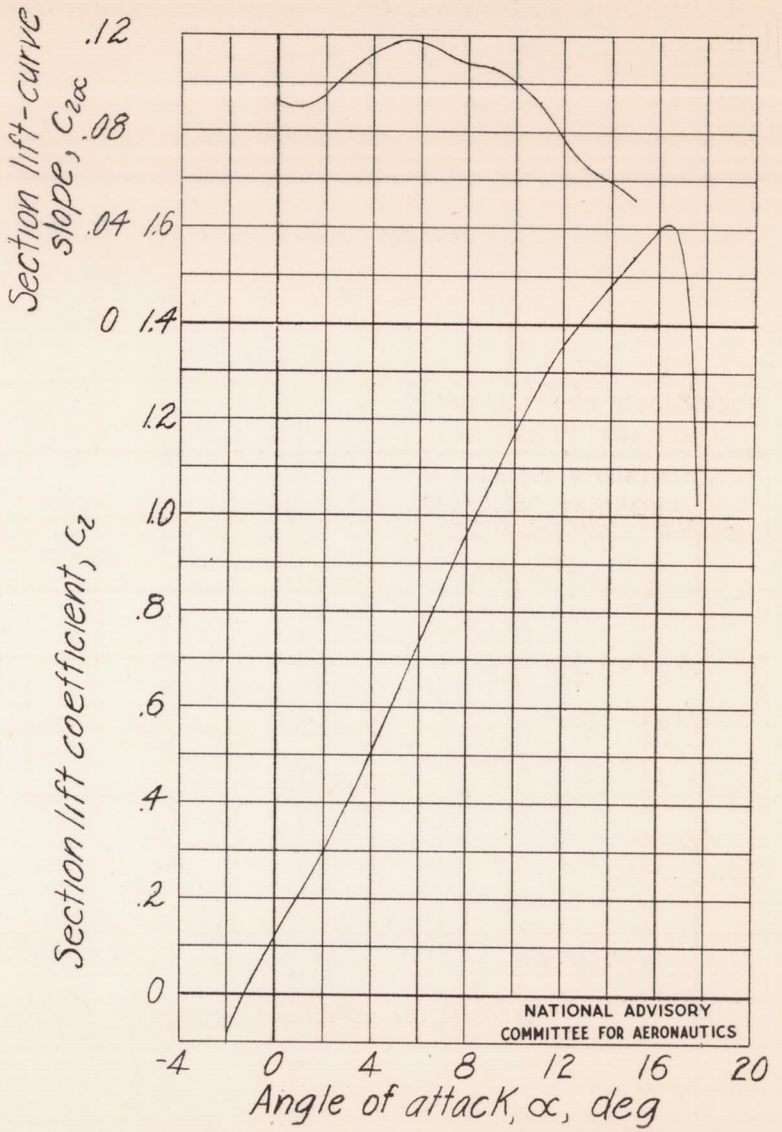

(b) Rectangular wing; NACA 23012 airfoil section.

Figure 10.- Section lift characteristics of wings tested. $\frac{pb}{2V} = 0$; $\psi = 0^\circ$; $R = 3 \times 10^6$.

(Data from Langley two-dimensional low-turbulence tunnel.)

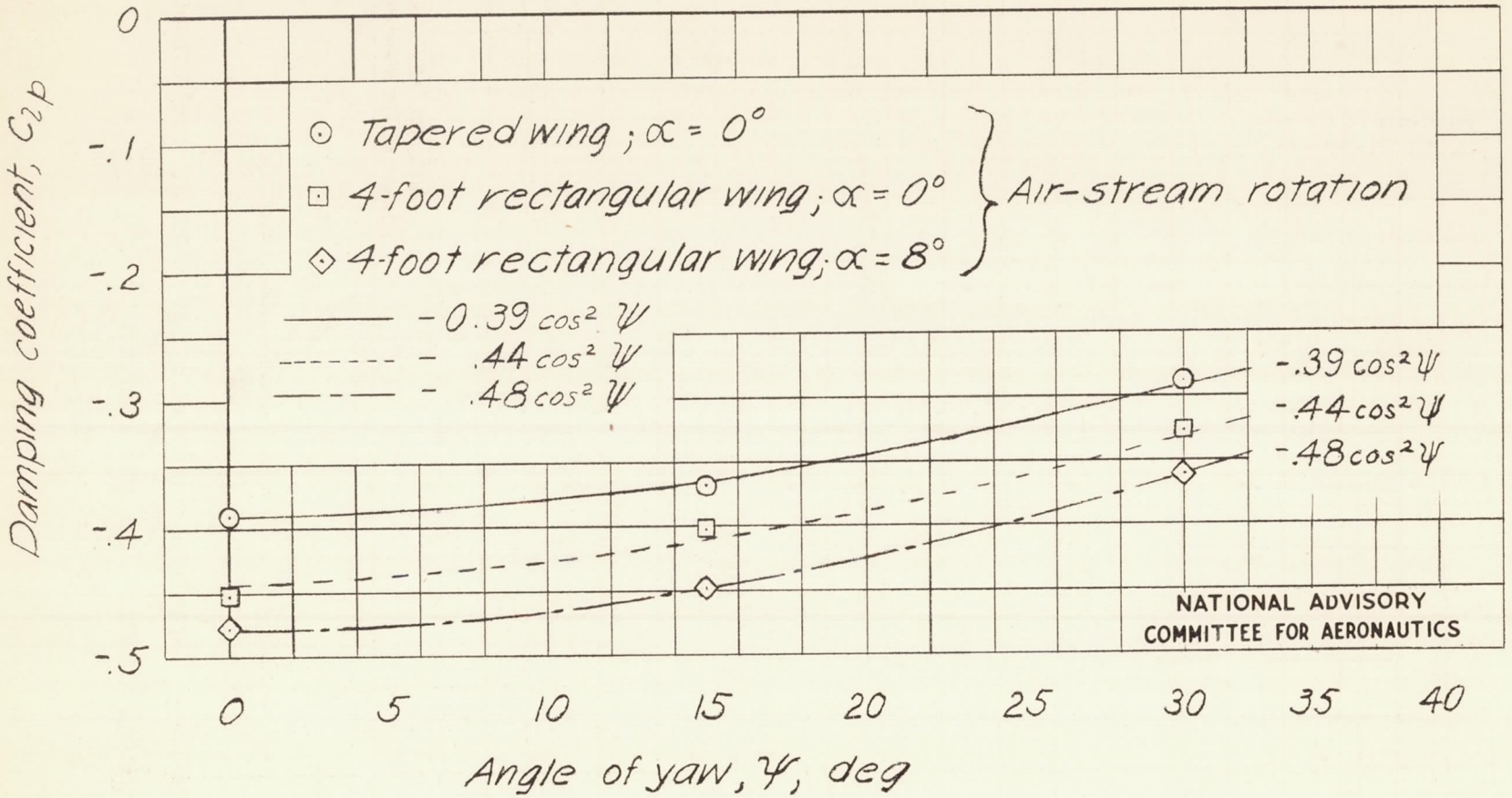

Figure 11.- Variation of damping in roll with angle of yaw.

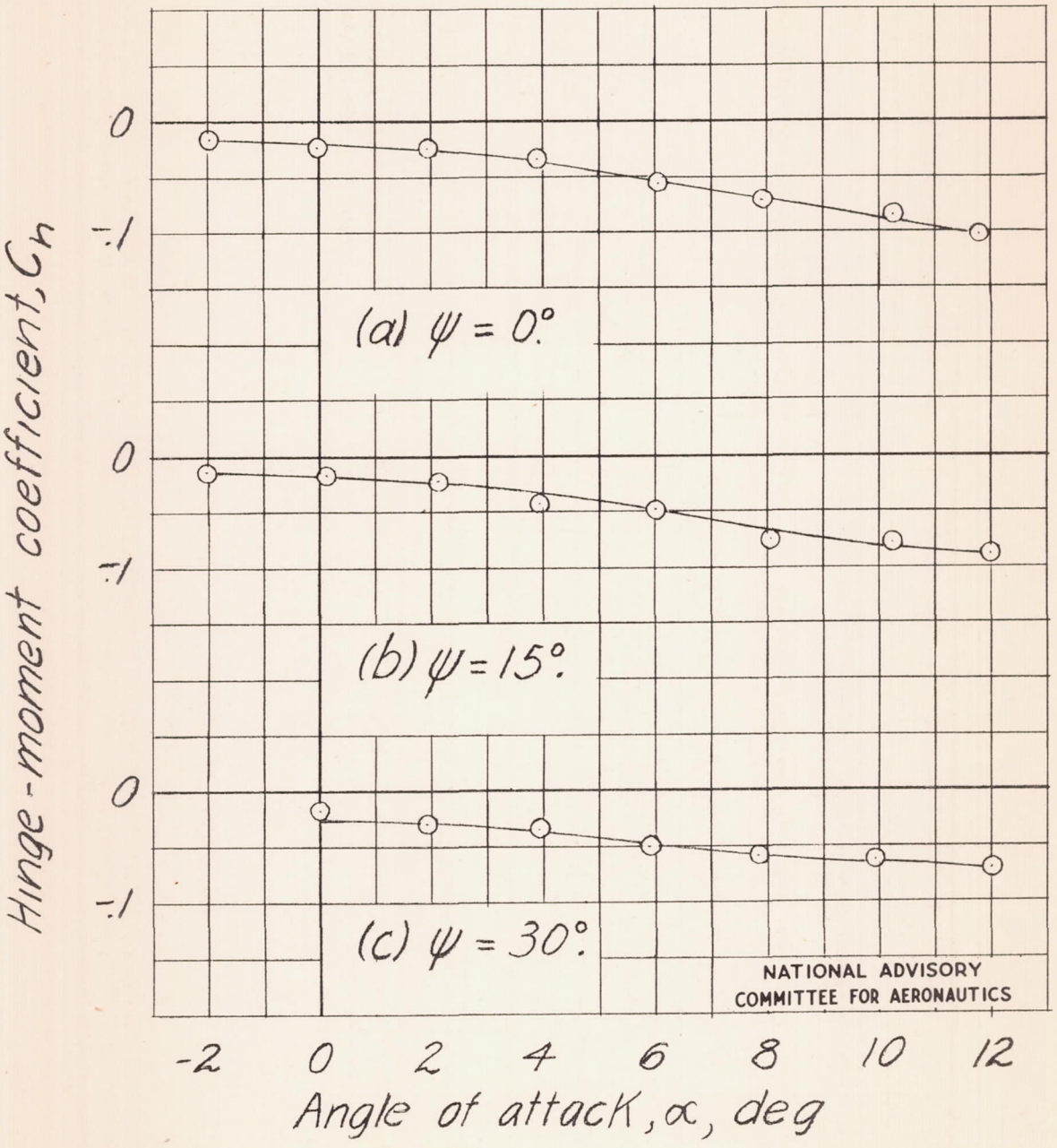

Figure 12.- Variation of aileron hinge-moment coefficient with angle of attack. Tapered wing; $\delta_a = 0°$; $\frac{pb}{2V} = 0$.